All Sciences Proceedings

1st International Conference on Contemporary Academic Research

May 17-19, 2023 : Konya, Turkey

ICCAR

All Sciences Proceedings
http://as-proceeding.com/

https://as-proceeding.com/index.php/iccar

PID control of a zero stiffness magnetic suspension system

Ergin Kılıç*, Berkan Kuşcu

[1]Department of Mechanical Engineering, Suleyman Demirel University, Turkey
[2]Department of Mechanical Engineering, Suleyman Demirel University, Turkey

*erginkilic@sdu.edu.tr

Abstract –As a result of the developments in today's technology, magnetic suspensions have started to be used instead of traditional suspensions (mass-spring-damper) in order to prevent vibrations in structures. In conventional suspensions, there is an undesirable continuous force transfer from the ground to the user according to the action-reaction principle of the existing spring and damper used in the suspension system. Although the mass-spring-damper parameters are well adjusted in a conventional suspension, this transmitted force transfer cannot be reduced to zero. The main purpose of this study will be a magnetic suspension design to eliminate this undesirable situation. In the designed magnetic suspension, the magnet on the linear guide system will be tried to be kept in the zero transmitted force position with the help of only magnetic forces without any mechanical contact and lubrication. A total of 3 magnets will be used in the proposed magnetic suspension system. The magnet on the linear guide will be capable of free sliding and this sliding magnet will be actuated by the rotary magnets standing in a fixed position at ends of the linear guide system by using the repulsive or pulling forces. The position control of the sliding magnet is achieved by a PID control. Therefore, since no mechanical spring and damper connections will be used in the proposed suspension system, zero spring force effect could be created.

Keywords – Magnetic Suspension, Magnetic Forces, Zero Stiffness, PID Position Control.

I. INTRODUCTION

In traditional suspension systems, there are spring and damping elements, and the unwanted force values transmitted to the passenger increase as the spring move away from the balance point. With the advancement of technology, magnetic suspensions have started to be used instead of traditional suspensions due to their advantages such as non-contact operation, elimination of friction forces and gravity balancing. Mathematical modeling of the Magnetic Levitation (Mag-Lev) system and position control studies in a 10 mm air gap with the feedback linearization method of this system are known [1]. In another Mag-Lev study, an iron ball was found to follow various reference commands in a 10 mm air gap using the adaptive control law [2]. Position control studies of a ball in 20 mm air gap were carried out with fuzzy logic based PID controller study [3]. There are also studies in which Mag-Lev systems can be modeled using neural networks and position control is provided in a 30 mm air gap [4]. Although all these studies are called magnetic suspension in the literature, the position of the electromagnets used is fixed relative to the ground and ground excitation tests have not been performed. In particular, the effect of excessive non-linear magnetic forces, which will occur when the mass suspended in the air by an excitation from the ground, approaches the stationary electromagnets rapidly, has not been observed. If the relative position of the suspended mass is very close to the electromagnet, unstable situations occur because the magnetic forces will rise to extremely high levels. Therefore, it can be seen that suspended masses can only be controlled up to a limited value of the air gap. In this study, instead of using current-

controlled permanent electromagnets, a magnetic suspension system with a unique design that can work stable up to half the air gap is proposed by using natural magnets with rotational movement.

II. Materials and Method

In the system shown in Fig. 1, there are 3 Neodymium (N35) magnets with dimensions of 50×50×25 mm, the middle magnet can only slide freely, and the magnets at the other two ends are rotated at the desired angle with the help of DC motors. In this way, it is aimed to move the sliding magnet to the desired position by utilizing the repulsion-pulling forces of the magnets to each other. The DC electric motors used are 30:1 with metal gearbox, operating voltage: 12V, no load speed: 350rpm, stalling torque: 0.77 Nm, stalling current: 5A and its mechanical output power is around 7 Watts. The linear position of the sliding magnet is read with the help of an encoder (1024 ppr) connected to a slider-crank mechanism. In order not to be affected by the magnetic field, the slide shafts are made of brass material and the other parts are made of aluminum material as shown in Fig. 2.

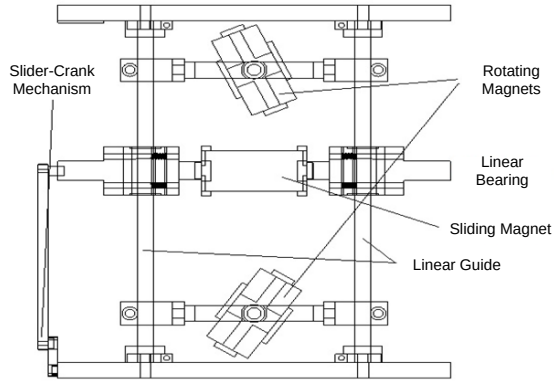

Fig. 1 Schematic of the magnetic suspension system

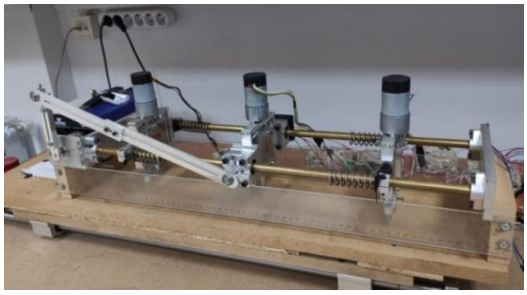

Fig. 2 View of the experimental setup.

A. Calculation of magnetic forces

With the help of an empirical formula suggested by Reference [5], the magnetic forces depending on the distance (γ) and angle (θ) between two cubic magnets can be easily calculated as shown in Eq. 1.

$$F_m = sin\theta . A/(B+\gamma)^n \quad (1)$$

The force (F_m) values corresponding to the different γ and θ values on the experimental setup were determined as shown in Fig 3, and the *A*, *B* and *n* parameters that would best fit this data set were determined as shown in Table 1.

Table 1. Best fit parameters for Eq.(1)

n	***A***	***B***
3,9758	0,0041	0,0227

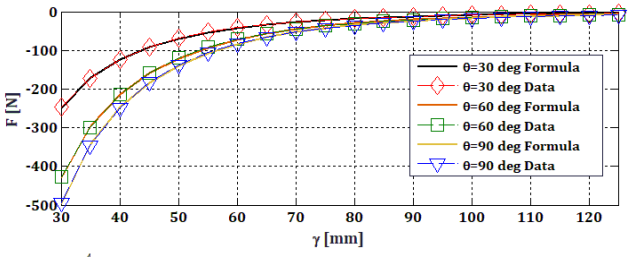

Fig. 3 Verification of the optimized parameters for magnetic force calculations

B. Free Vibration Tests

In the configuration suggested by Reference [6], there are two magnets repelling each other. By deactivating the rotating magnet above in the experimental setup system shown in Fig 4, the accuracy of the mathematical model developed on two magnets will be observed.

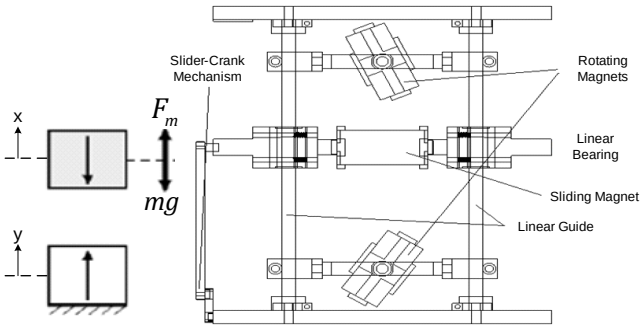

Fig. 4 Free vibration test.

The expression of the mathematical model used is given in Eq. 2.

$$m\ddot{x} + c\dot{x} = F_m - mg \tag{2}$$

Firstly, after 1 cm input is given to the sliding magnet, the displacement values read until it reaches the equilibrium position are shown in Fig 5. The time values of the peak points of the waves are given in Table 2. The amplitude differences of the wavelengths are also given in Table 3.

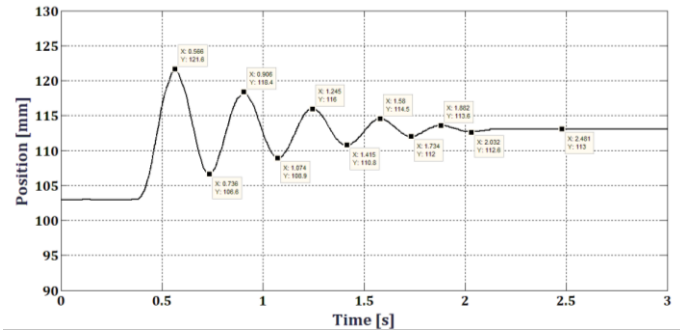

Fig. 5 Free vibration obtained by giving 1 cm input.

Table 2. Time values of the peak points of the waves.

$t_1 = 0{,}566\ s$	$t_2 = 0{,}906\ s$	$t_3 = 1{,}245\ s$	$t_4 = 1{,}58\ s$	$t_5 = 1{,}882\ s$
$t_{1.5} = 0{,}736\ s$	$t_{2.5} = 1{,}074\ s$	$t_{3.5} = 1{,}41\ s$	$t_{4.5} = 1{,}734$	$t_{5.5} = 2{,}032\ s$

Table 3. Amplitude differences of wavelengths.

$x_1 = 121{,}6 - 113 = 8{,}6$	$x_{1.5} = 113 - 106.6 = 6{,}4$
$x_2 = 118{,}4 - 113 = 5{,}4$	$x_{2.5} = 113 - 108{,}9 = 4{,}1$
$x_3 = 116 - 113 = 3$	$x_{3.5} = 113 - 110{,}8 = 2{,}2$
$x_4 = 114{,}5 - 113 = 1{,}5$	$x_{4.5} = 113 - 112 = 1$
$x_5 = 113{,}6 - 113 = 0{,}6$	$x_{5.5} = 113 - 112{,}6 = 0{,}4$

Logarithmic decay rates of the wavelengths are calculated as shown in Eq. 3.

$$\delta_{1-2} = \ln\left(\frac{x_1}{x_2}\right) = \ln(1{,}592) = 0{,}4649 \tag{3}$$

Eq. 4 shows the damping ratio values;

$$\zeta_{1-2} = \frac{\delta}{\sqrt{\delta^2 + 4\pi^2}} = \frac{0{,}4649}{\sqrt{0{,}4649^2 + 4\pi^2}} = 0{,}0737 \tag{4}$$

The natural frequency is calculated by the help of Eq.5;

$$w_{n1-2} = \frac{2\pi}{T_d \cdot \sqrt{1-\zeta^2}} = \frac{2\pi}{(0.906 - 0.566) \cdot \sqrt{1 - 0{,}0737^2}} = 18{,}53\ \text{rad/s} \tag{5}$$

The value of the critical damping is given in Eq. 6;

$$c_{c1-2} = 2 \cdot m \cdot w_n = 2 \cdot 1{,}6 \cdot 18{,}53 = 59{,}296\ \ \text{N} \cdot \text{s/m} \tag{6}$$

The value of the damping coefficient is calculated by Eq.7;

$$c_{1-2} = \zeta \cdot c_c = 0{,}0737 \cdot 59{,}296 = 4{,}37\ \ \text{N} \cdot \text{s/m} \tag{7}$$

The value of the spring coefficient is found by using Eq. 8;

$$k_{1-2} = m \cdot w_n^2 = 1{,}6 \cdot 18{,}53^2 = 549\ \ \text{N/m} \tag{8}$$

All of the values given in Table 2 and Table 3 are recalculated similar to the calculations in Eqs. 3-8 and it is found that the spring constant (*k*) of the magnetic system is between 549-726 *N/m*, the damping coefficient (*c*) is between 4.37 – 9.83 *N.s/m* and the natural frequency (ω_n) is around 18,53 – 21.30 *rad/s*.

C. Simulation Study

The parameters obtained from the experimental data will be verified by modeling on MATLAB/Simulink. A study was carried out by giving 10 mm input from the ground (y position) to the magnetic suspension system created in the simulation environment. The force formula given in Eq. 1 was used to calculate the magnetic force of the magnets. It should be emphasized that the $h_1 = \gamma$ defined in the simulation model is taken as the distance from the midpoints of the magnets to each other ($|x - y|$).

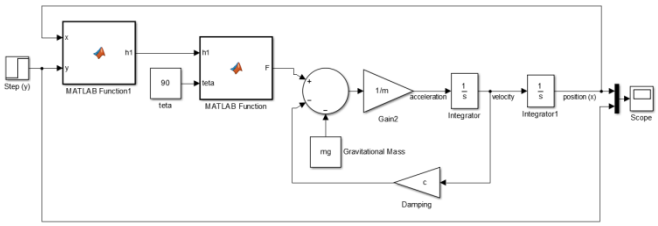

Fig. 6 MATLAB/Simulink model of the suspension system.

Different damping coefficients in the range of [4.37 - 9.83] were tried on the model created in Fig. 6, and it was seen that the most compatible output, which would match the experimental results, was obtained when the damping coefficient was used as 5 $N{\cdot}s/m$. As seen in Fig. 7, although the number of vibration cycles is high in the simulation output, it is seen that the vibration amplitudes almost overlap. The most important reason for this inconsistency is that while there is dry friction in the real system, the viscous friction model is used in the simulation system.

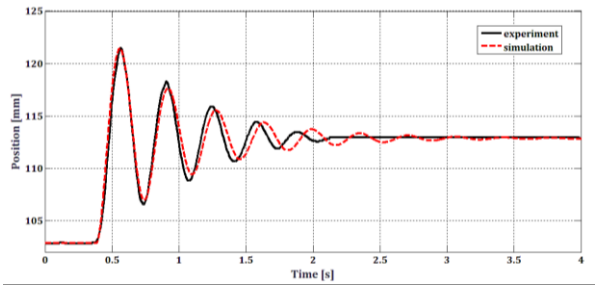

Fig. 7. Verification of the experimental and simulation results

D. *Position control of the magnetic suspension system*

The schematic representation of the magnets whose position control will be implemented is shown in Fig. 8. As can be seen, the position of the magnet in the middle will be determined by utilizing the repulsion and attraction forces of the same and opposite poles of the magnets. The angle of the magnet in the middle will be fixed at 90 degrees and will slide in +h and -h directions. The magnets in the upper and lower positions will only make a rotational movement, allowing the middle magnet to move in the ±h directions.

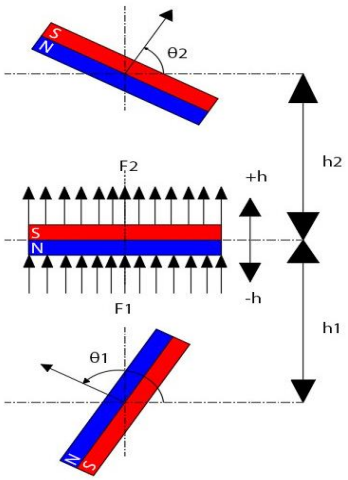

Fig. 8. Position control of the magnetic suspension system.

The distance of the permanent magnets to each other is set as $h_1 + h_2 = 0{,}24\,m$. Therefore, the distances of the sliding magnet, which has a total mass (m) of 1.6 kg with the connection equipments, is determined to the permanent magnets as $h_1 = |x - y|$ and $h_2 = 0.24 - |x - y|$. Since both permanent magnets are θ_1=θ_2=45° at the initial time, the sliding magnet is in an equilibrium position 0.101 m above the lower permanent magnet ($h_1 = 0.101$ m). It should be noted that the angle values θ_1 and θ_2, which will take place in Eq. 1, are allowed to be minimum -90° and maximum +90°. The reason why the initial angle values are 45° is that the sliding magnet is allowed to move up or down from its equilibrium position. Thus, the designed magnetic suspension system could be controlled for a desired reference $r(t)$ either up or down. As shown in Fig. 9, a PID control design has been made to control the relative motion ($|x(t) - y(t)|$) of the sliding magnet with respect to the permanent magnet at the bottom. It should be noted that while the PID controller calculates the θ_1 and θ_2 angles as equivalent, as shown in Eq. 9, the error that will occur according to the reference position is defined as $e(t) = r(t) - |x(t) - y(t)|$.

$$\theta_1 = \theta_2 = K_p.\,e(t) + K_i \int_0^t e(t)\,dt + K_d \frac{de(t)}{dt} \qquad (9)$$

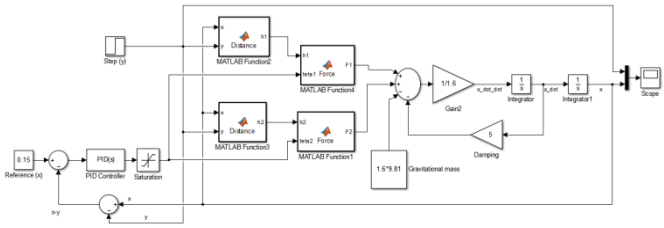

Fig. 9 PID control of the magnetic suspension system.

III. RESULTS

In the realized PID control design, K_p coefficient is set to 3689, K_i coefficient is 4255 and K_d coefficient is set to 447. The results obtained while traveling from the equilibrium position of the sliding magnet ($h_1 = 0.101$ m) to the desired reference values of $r = |x - y| = 0.15\,m$ and $r = |x - y| = 0.05\,m$, respectively, are presented in Fig 10. In the simulation study, after the 5th second, a disturbance input with a unit step input of 0.01m amplitude from the ground is also applied. Even if there is a disruptive input, it is seen that the sliding

magnet can successfully maintain its reference value ($r = |x - y|$) continuously. Fig 11 shows how the rotating magnet angles ($\theta = \theta_1 = \theta_2$) change momentarily.

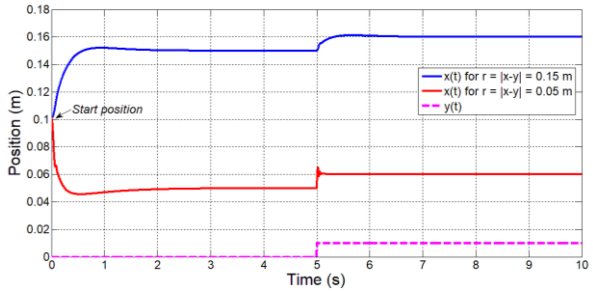

Fig. 10 Simulation results for the position of the sliding magnet.

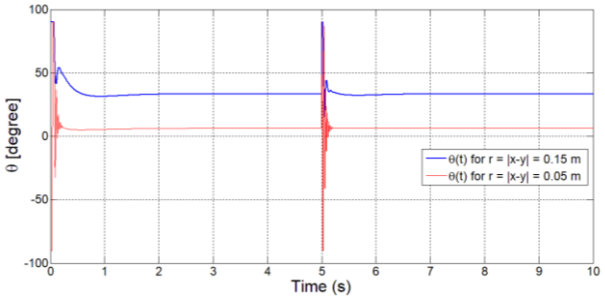

Fig. 11 Simulation results for the angle of the rotary magnets.

After successful results were obtained in the simulation study, trial tests were started on the real test platform. However, the actual experimental system was operated in a horizontal configuration, not vertically, as shown in Fig 2. In addition, the distance between two fixed rotating magnets has been drawn to a wide range such that $h_1 + h_2 = 0{,}4\ m$. PID control coefficients have been updated to be K_p = 4000, K_i = 2000 and K_d = 500, and the results are presented in Fig 12. The sliding magnet is located in the middle of the two permanent magnets in the bed position and the starting point is accepted as 0 mm. In other words, the position values presented in Fig 12 correspond to the expression $\pm h$.

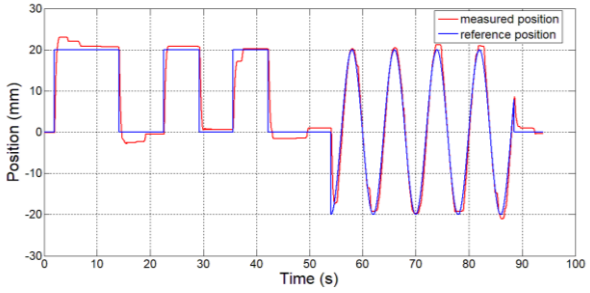

Fig. 12 Experiment results for the position of the sliding magnet.

IV. DISCUSSION

When the working performance of the PID controller is examined from the simulation results, it is seen that sliding magnet goes to the target position by 4% overshoot within 2 seconds of settling time and with 0 steady state error. In the experimental results, it is seen that the settling time of the PID controller performance is 5 seconds, the overshoot is around 10%, and the steady state error is below 1 mm.

V. CONCLUSION

In this study, a magnetic suspension system with precise position control was realized and after free vibration experiments, a simple simulation modeling was carried out on the parameters obtained and preliminary tests were made on the developed experimental setup. However, in order to be applied to a real vehicle, larger magnets must be used. In addition, the reason why a precise position control is provided in theory (i.e. in the simulation environment) but this cannot be achieved in the experimental results is the power deficiency of the 7 Watt DC motors controlling the rotating magnets, and it has been seen that in theory, it cannot go to the angular position instantly without error. Therefore, in future studies, if practical application in vehicles is considered, it is recommended to use hydraulic motors with high speed and torque capacity or use of more powerful electric motors.

ACKNOWLEDGMENT

The experimental setup used in this study was created in the master's thesis of Berkan KUŞÇU [7], supervised by Associate Professor Ergin KILIÇ.

REFERENCES

[1] S. Öztürk, S. Kizir, Z. Bingül, and C. Oysu, "Manyetik süspansiyon sisteminin gerçeklenmesi ve kontrolü," *TOK 2007*, pp. 95–100, Turkey.

[2] N. Sun, Y. Fang, and H. Chen, "Tracking control for magnetic-suspension system with online unknown mass identification," *Control Engineering Practice.*, vol. 58, pp. 242–253, 2017.

[3] M. Golob and B. Tovornik, "Modeling and control of the magnetic suspension system," *ISA Transactions.*, vol. 42, pp. 89–100, 2003.

[4] R. Jesus, L. Zhang, E. Lughofer, P. Cruz, A. Alsaedi and A. Hayat, "Modeling and control with neural networks for a magnetic levitation system," *Neurocomputing.*, vol. 227, pp. 113–121, 2017.

[5] W.S. Robertson, M.R.F. Kidner, B.S. Cazzolato and A.C. Zander, "Theoretical design parameters for a quasi-zero stiffness magnetic spring for vibration isolation," Journal of Sound and Vibration, vol. 326, pp. 88-103, 2009.

[6] W. Robertson, R. Wood, B. Cazzolato and A Zander, "Zero-stiffness magnetic springs for active vibration isolation," International Symposium on Active Noise and Vibration Control, 2006, Australia.

[7] B. Kuşcu, "Vehicle Suspension Control with Magnetic Force," M. Sc. Thesis, Süleyman Demirel University Graduate School of Natural and Applied Sciences Department of Mechanical Engineering, Isparta, Turkey, 2022.